ORIGINAL ARTICLE

Evaluation of milling performance of 50-µm D-shaped carbide tool, polycrystalline diamond-coated carbide tool, and polycrystalline diamond tool

Jin Xin Jiang[1] · Chen Jiang[1] · Rui Gao[1] · Yu Hao[1]

Abstract

Tool sizes and material properties significantly influence the surface quality of micro grooves and the life of the milling tool in micro milling. Thus, expanding the application range of micro-milling tool sizes and exploring the milling performance of different materials are crucial for high-precision milling. In this study, the experimental research on in situ preparation and in situ milling was conducted using a self-developed high-precision combination machine tool. The preparation of D-shaped micro-milling tools with a diameter of 50 µm class was realized using a wire-cutting electrical discharge grinding technology. The performances of carbide, polycrystalline diamond (PCD)-coated carbide, and PCD tools during the micro-milling process of brass were investigated in terms of tool wear and workpiece surface finish. The results showed that the PCD micro-milling tool had the slightest wear, effectively inhabited burr generation, and had stable side wall and groove bottom processing capabilities compared with uncoated and coated PCD carbide micro-milling tools. In addition, the surface roughness of the PCD micro-milling tool was 41.9% lower than that of the carbide micro-milling tool, and high-precision machining with minimum roughness of 32.37 nm was realized. PCD micro-milling tool had excellent milling properties, which significantly prolonged tool life and improved machining quality and accuracy.

Keywords PCD coating · D-shaped micro-milling cutter · Wire electrical discharge grinding · Surface morphology

1 Introduction

Micro-milling has attracted considerable attention owing to its high precision, high machining efficiency, three-dimensional machining capability, and wide range of workpiece materials [1, 2]. With the development and progress in science and technology, the precision requirements of micro and small parts are getting higher and higher [3]. A higher precision in the size of the micro-milling tool is required to meet the miniaturization and three-dimensional particularity of machining parts. Many researchers have worked on the preparation and application of micro-milling tools within a diameter range of 100–500 µm and investigated the wear behavior of micro-milling tools of different diameters (500 [4], 300 [5], 200, and 152.4 µm [6]) during micro milling and their effects on surface quality. Studies have shown that small-size tools can improve machining accuracy and milling performance. However, small-size tools can have high stress deformation and even fracture failure due to poor stiffness and edge strength [7, 8]. Therefore, optimizing the tool geometry to improve the micro-milling tool resistance to edge deformation and damage during micro-milling applications is necessary. Chen et al. [9] reported that straight edges were more prevalent during the preparation of micro-milling tools with a diameter of less than 200 µm owing to their high stiffness and ease of manufacture. Uhlmann et al. [10] optimized the tool geometry using the finite element method analysis. They reported that simple geometry (such as no helix) was more suitable for micro-milling tools with a diameter of less than 50 µm. Compared with the traditional spiral milling tool, the micro-milling tool with a simple shape had higher bending stiffness and strength with decreased machining size in the micromachining process. In addition, circular, D-shaped, triangular, and square tools exhibited different micromachining performances.

✉ Chen Jiang
  jc_bati@163.com

1   College of Mechanical Engineering, University of Shanghai
    for Science and Technology, Shanghai 200093, China

D-shaped tools have better performance in surface finish, tool wear, and cutting force, and they can be used to improve the accuracy of ultra-precision manufacturing [11].

Tool failure caused by tool wear negatively affects the surface integrity and machining accuracy of micro-milling workpieces [12, 13]. The rapid wear of tools is inevitable, especially for micro-milling tools. As the tool size decreases, the probability of wear increases, which is a significant problem that needs to be urgently solved in micro milling [14]. Material properties significantly affect the life cycle of a tool. Thus, to improve machining accuracy and extend the life cycle of a tool, the study of the milling performance of tools with different characteristics is necessary. Diamond has been reportedly considered one of the most suitable materials for micro-milling tools owing to its superior hardness and wear resistance [15]. Zhao et al. [16] prepared a chemical vapor deposition diamond (CVD) micro-milling tool via the composite process. The results showed that the CVD tool had fewer burrs than the carbide tool, and the minimum surface roughness was 53 nm. Wang et al. [17] compared the cutting performance of nano polycrystalline diamond (NPCD) tool with that of single crystal diamond tool in machining SiC molds. They found that the surface texture processed using the NPCD tool was more pronounced. Diamond materials significantly improve tool milling performance, especially polycrystalline diamonds. Thepsonthi et al. [18] pointed out that PCD maintained high hardness and toughness at high temperatures. Kolar and Masek [19] investigated the service life of the tool. Based on the side wear of 0.1 mm, they found that the wear of the PCD tool was one-sixth of that of coated carbide tool. Cheng et al. [20] designed a geometrically symmetric PCD micro hexagonal end mill with a diameter of 450 μm. The axial forward angle, axial clearance angle, and radial forward angle were equal. The newly designed hexagonal end milling tool had high-quality machining of the side and bottom of the workpiece, making the roughness reach the submicron level.

Generally, wear resistance and surface finish are important indicators for evaluating tool performance. The hard coating significantly increases tool life and reduces surface roughness owing to the superior mechanical and friction properties of the tool [21]. To study the effect of DCL deposition on the milling performance of carbide tools, Cheng et al. [22] plated a layer of DCL on cemented carbide-forming tools. They found that the hardness of the coated tool increased by 17%, and the wear resistance of the tool significantly improved. In addition, Atlanta et al. [23] studied the effects of nano-diamond (NCD), TiN, and AlCrN coating and uncoated carbide tools on tool wear and rough edge size in the micro-milling of Ti6Al4V alloy. The results indicated that the NCD-coated tool exhibited the slightest wear and burr size. Liang et al. [24] studied the cutting performance of micro-milling tools with different coatings during the machining of Ti-6AI-V alloy. Compared with the uncoated micro-milling tool, the AITIN-based coating reduced the chip and tool wear length on the cutting edge, thereby prolonging the service life of the tool. Researchers compared the milling performance of the AlTiN-coated, PVD-coated, and uncoated WC tools in terms of roughness values and burr widths and found that the AlTiN-coated tool had lower roughness values and burr widths [25].

Currently, a micro-milling tool with a minimum size of 100 μm is mainly used in many applications. The tool head size prepared with high-hard materials cannot meet the ideal machining accuracy. Thus, to further expand the application range of micro-milling tool size and prolong tool life, in this study, the micro-milling tool with a 50 μm diameter was prepared using wire-cutting electrical discharge grinding (WEDG) technology on the self-developed μEM-200CDS2 high-precision machining machine. In addition, the milling experiments were conducted on different stations of the same machine. By comparing the uncoated and coated PCD carbide tools, the cutting performance of the PCD tool during the milling of brass was studied. Scanning electron microscopy (SEM) and ultra-depth-of-field microscopy were used to examine burrs, tool wear, and surface morphology. The tool wear and groove bottom morphology of the uncoated and coated PCD carbide tools were analyzed. The width, depth, profile, and surface roughness of the microgrooves during the milling process were subsequently measured and analyzed to obtain tools with longer service life and better cutting performance in micro milling.

2 Equipment test and milling scheme

2.1 Fabrication of cutting tool

The experiments were performed on different stations on the same micro EDM machine. The basic principle is shown in Fig. 1. On the self-developed μEM-200CDS2 machine, the micro-milling tool blanks were clamped to the spindle, and the micro-milling tool was prepared using WEDG technology on station I. The spindle was moved to station II without removing the cutter to start the micro-milling experiment.

Figure 2 illustrates the experimental platform, milling process, and tool structure. The D-shaped carbide, PCD-coated, and PCD tool were prepared using wire electrode WEDG on the self-developed μEM-200CDS2 machine and milled in situ. The minimum linear feed in the Z-axis was 0.1 μm, and the spindle radial runout accuracy was 1 μm. As shown in Fig. 2a, the cutting fluid removed the chips from the cutting area and reduced the temperature. During preparation, the tool was clamped on the high-speed spindle, and the servo motor controlled the rotation of the insert in the direction shown in Fig. 2b. Figure 2c shows a schematic view of the
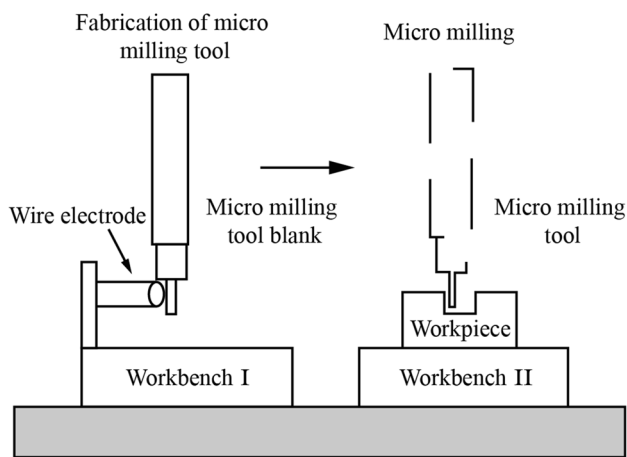
Fig. 1 Schematic diagram of in-situ preparation and application of WEDG-based micro-milling tool

micro-milling process. The size characteristics of the prepared D-type tool head are shown in Fig. 2d, and the diameters of the handle D and D1 were 3 and 0.05 mm, respectively. Cutting edge length L_1 and tool length L were 0.15 and 30 mm, respectively, and the cutting edge inclination γ

and half cone angle β of the cutter neck were 20° and 15°, respectively. The tool diameter was measured using scanning electron microscopy. The diameters of the carbide tool, PCD-coated tool, and PCD tool were 50, 56, and 45 μm, respectively. The thickness of the PCD coating was 1 μm.

2.2 Milling schemes

Ultra-fine grain carbide and polycrystalline diamond were used as micro-milling tool materials in the experiment owing to their high hardness, high wear resistance, and high bending stiffness. Table 1 shows the main parameters of carbide, diamond coating, and PCD materials.

Three sets of tools were tested with the same milling parameters, with each set of tools milling five straight grooves. The length of each microgroove was 3 mm, and the milling length of 15 mm was finally achieved in each group of experiments. Table 2 shows the milling parameters of the milling experiment. The milling depth per feed was 0.002 mm, and the total milling depth for microgrooves milled using the uncoated and coated carbide tool was 0.01 mm. The surface of the workpiece was cleaned using an ultrasonic machine after it was processed. The surface morphology of the microgroove

Fig. 2 Micro-milling tool fabrication and on-machine micro-milling processing of the μEM-200CDS2 machine tool. (**a**) On-machine micro-milling tool fabrication with WEDG; (**b**) Rotation direction of the tool head (micro-milling); (**c**) Micro-milling process; (**d**) Front view (left) and right view (right) of D-type tool head
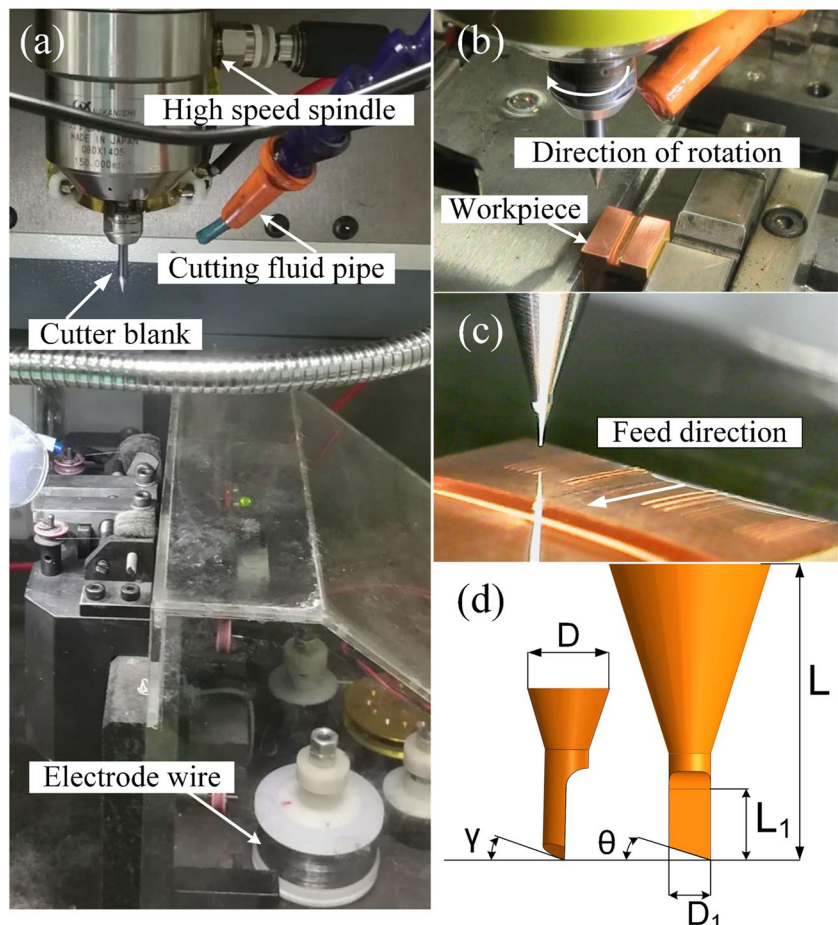
Table 1 Material parameters

Project	Carbide	Diamond coating	PCD
Density ρ /(g*cm^{-3})	14.40	4.3	4.3
Elastic modulus E /(GPa)	800	890	890
Poisson's ratio μ	0.22	0.07	0.07
Hardness H_V /(MPa)	1900	10000	10000
Grain size Z_v /(μm)	0.4	0.5	0.5
Co-content (%)	9	15	15
Bending strength	4000	1500	1500

Table 2 Milling parameters

Cutting cutters	Carbide	Diamond coating	PCD
Spindle speed n / (r/min)	150,000	150,000	150,000
Feed rate per tooth f_t /(μm)	0.02	0.02	0.02
Cutting depth a_p / (mm)	0.002	0.002	0.002
Flushing speed v / (mm/s)	100	100	100
Number of processing layers	5	5	10

bottom was analyzed using a scanning electron microscope. The surface roughness of the groove bottom was measured using a white light interferometer along the feed direction.

3 Experimental results and analysis

3.1 Experimental results

3.1.1 Microgrooves

Figure 3 shows the surface morphology of microgrooves milled using a PCD-coated carbide tool at different milling distances. Some black spots on both sides of the microgroove were attributed to the particles generated from the brass workpiece during the milling process. As shown in Fig. 3a, the bottom of the microgroove was smooth and flat, owing to the sharpness of the tool to effectively cut the material at the initial stage of milling. When microgrooves were milled to the second groove, the coating adhered to the tool head was milled out with two noticeable linear scratches at the bottom of the groove formed due to the uneven wear of the coating on the cutter head (Fig. 3b). As shown in Fig. 3c, no apparent linear scratch was observed at the bottom of the groove. However, the plowing phenomenon occurred during milling. As shown in Fig. 3d, e, the cutting thickness at the bottom of the microgroove reduced and formed an arc shape due to the severe wear of the PCD-coated carbide tool with the increased milling distance.

Figure 4 shows the SEM images of surface burrs milled with different tools. Figure 4a shows the microgrooves milled using the carbide tool, and large burrs appear on the down-milling side. During the milling process, a part of the material entered the cutting end along the rake face under the extrusion of the tool, and the material was bent and broken on the lower milling surface to form burrs. In addition, the wear of the carbide tool made the uncut thickness less than the tip radius. A continuous change in chip thickness led to the accumulation of more deformed material on the down-milling side, resulting in larger burr sizes. As shown in Fig. 4b, the burrs of microgrooves milled with the PCD-coated carbide tool were significantly smaller than that of microgrooves milled with the carbide tool. This phenomenon is because the Co content affects the edge strength of the blade. The Co content in PCD was higher than that of cemented carbide. The high content of Co in PCD endowed the PCD-coating tool to maintain its original sharpness and achieve effective cutting. As shown in Fig. 4c, the burr sizes of microgrooves milled with the PCD tool were similar to that of the PCD-coated carbide tool, but the distribution of burrs of microgrooves milled with the PCD tool was more uniform.
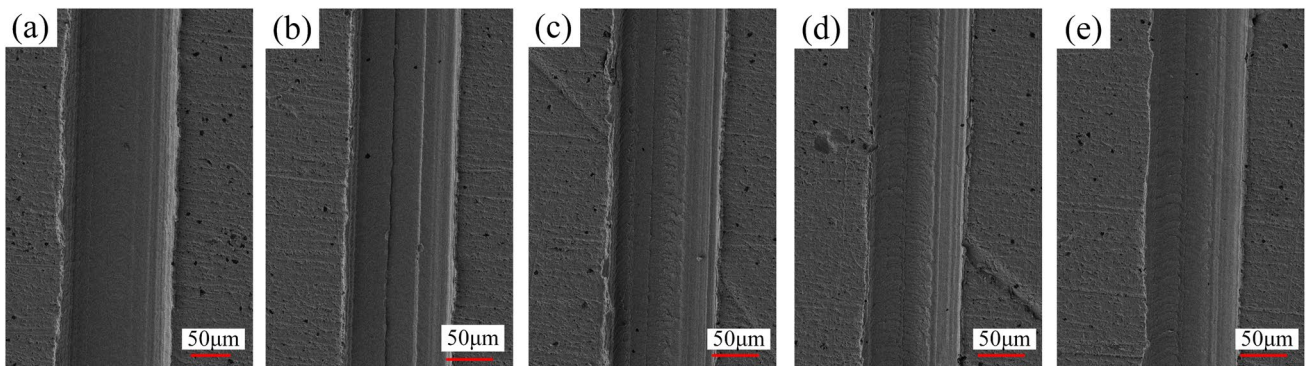
Fig. 3 Surface morphology of microgrooves milled with PCD-coated carbide tool. (**a**) First straight groove; (**b**) Second straight groove; (**c**) Third straight groove; (**d**) Fourth straight groove; and (**e**) Fifth straight groove

Fig. 4 Burr morphology of the third microgroove (**a**) Carbide tool; (**b**) PCD-coated carbide tool; and (**c**) PCD tool
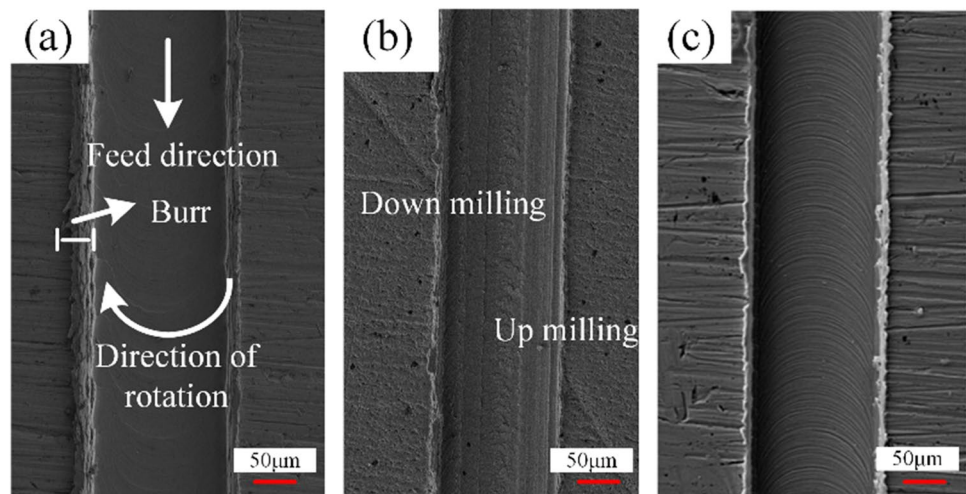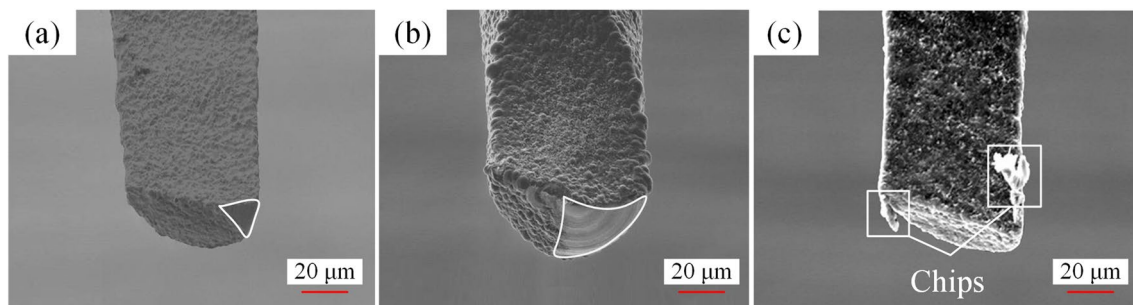

3.1.2 Tool wear

Figure 5 shows the wear degree of the carbide, PCD-coated carbide, and PCD tools. As shown in Fig. 5a, the tip of the carbide tool was severely worn after machining. The top of the contact surface between the tool and the workpiece was worn and became a wedge shape, which was uniformly distributed. A thick boundary line was observed between the worn and unworn area at the bottom of the PCD-coated carbide tool (Fig. 5b). Wear was slower in the areas with the coating than in areas without the coating, which caused maximum wear in the direction of the main cutting edge, resulting in a rounded bottom of the tool. Although the hardness of the coating material was higher than that of the carbide material, the wear area of the PCD-coated carbide tool was larger than that of the carbide tool. This phenomenon might be attributed to the following reason: when the coating was peeled off, the scratching between the exposed substrate material and the peeled coating at the bottom of the microgroove exacerbated the deterioration of the tool geometry. As shown in Fig. 5c, wear of the PCD tool almost did not occur on the tip. The chips still adhered to the surface of the cutting edge. Experimental results revealed that the PCD tool had longer service life than the uncoated and the PCD-coated carbide tool.

3.2 Microgroove surface morphology

3.2.1 Three-dimensional morphology

Figure 6 shows the three-dimensional at the different microgrooves. Figure 6a–c shows the bottom shape of the groove milled with the carbide tool. A shallow tool rotation trajectory occurred at the bottom of the microgroove. Several materials underwent elastic deformation under the extrusion at the bottom of the tool, accumulated on the back of the feed path, and concentrated on the cutting direction of the tool rotation, which became more significant with the increase in milling distance. Figure 6d–f shows the bottom morphology of the grooves milled out using a PCD-coated carbide tool. The groove in Fig. 5d has a relatively clear bottom. As the milling distance increased, the groove side wall locally remained uncut chips, forming two straight traces at the bottom of the microgroove (Fig. 6e). When the workpiece was milled to the end, the ratio of the undeformed cutting thickness to the cutting edge radius significantly reduced due to the deterioration of the tool tip geometry, resulting in the prevalence of plowing and reducing the surface quality of the microgroove (Fig. 6f). Figure 6(g–i) shows the groove

Fig. 5 Scanning electron microscope images of tool wear. (**a**) Carbide tool; (**b**) PCD-coated carbide tool; and (**c**) PCD tool
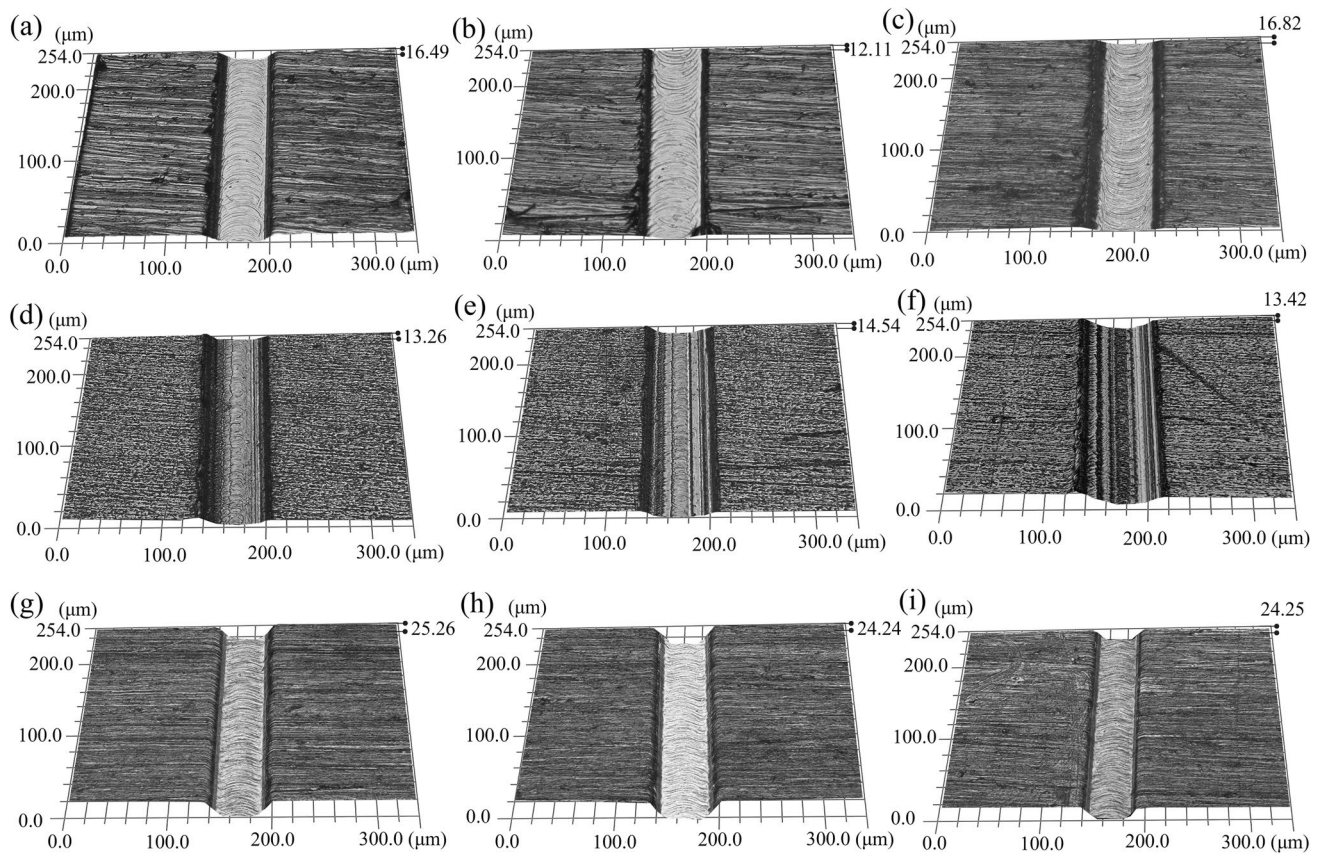
Fig. 6 The three-dimensional morphology of the microgrooves captured using the ultra-depth-of-field microscope. (**a–c**) First, third, and fifth groove bottom morphology milled with the carbide tool; (**d–f**) First, third, and fifth groove bottom morphology milled with PCD-coated carbide tool; (**g–i**) First, third, and fifth groove bottom morphology milled with PCD tool

bottom morphology of PCD tool milling. The tool path distribution was uniform and consistent in size, forming a fixed trajectory, indicating that PCD tools exhibited superior performance in microgroove surface morphology than uncoated and coated PCD carbide tools.

### 3.2.2 Groove width and depth

The maximum change rate can be used to evaluate the numerical stability of the changes in microgroove width and depth during the milling process. The maximum change rate calculation formula can be expressed as

$$\varphi_e = \frac{\max\left(\left|X_i - \bar{X}\right|\right)}{\bar{X}} \tag{1}$$

where φ_e represents the maximum rate of change; X_i represents the value point, $i = 1,2,3,4,5$; $\bar{X}$ is the average value; $\max\left(\left|X_i - \bar{X}\right|\right)$ represents the maximum absolute value of the difference between any value on the curve and the average value.

Figure 7a shows the variation in microgroove width with the milling distance of three different tool millings. When the milling distance was 2 mm, the microgroove width was close to the original diameter of the corresponding tool. The milling width of uncoated and coated PCD carbide tools increased with increasing milling distance, while the milling width of the PCD tool remained stable. During the whole milling process, the maximum change rates of microgroove width processed using the carbide, PCD-coated carbide, and PCD tools were 2.49, 8.84, and 0.18%, respectively. Figure 7b shows the variation in microgroove depth with milling distance under three kinds of tool milling. Due to tool wear and sharpness passivation, the microgroove depth of the carbide tool, PCD-coated carbide tool, and PCD tool gradually decreased with milling distance. The maximum change rates of the microgroove depth of the three tools were 9.6, 6.2, and 4.9%, respectively. Therefore, the PCD tool significantly improved the machining stability compared with the uncoated and coated PCD carbide tools.

Fig. 7 Variation in microgroove width and depth with milling distance. (**a**) Variation in microgroove width with milling distance; (**b**) Variation in microgroove depth with milling distance
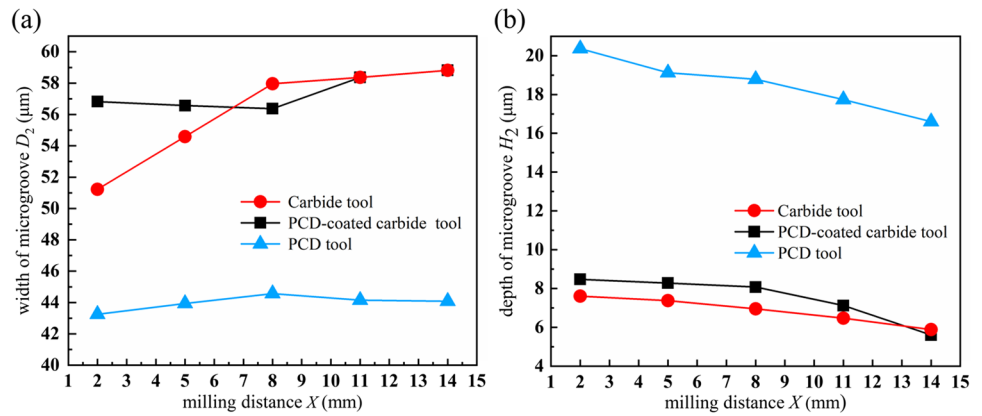
The microgrooves presented a reverse bone type because the wear at the bottom of the tool was greater than that at the top, making the shape of the tooltip evolve into an anticone and etching the microgroove during milling. As shown in Fig. 8a, the microgroove profile evolved from smooth and flat to the groove bottom bulge. The sidewall lost verticality; consequently, the microgroove contour deformation became severe. In addition, the tilt angle of the microgroove

was negatively correlated with the milling distance. Figure 8b shows that in the initial milling stage, the bottom of the groove is entire, and the side wall is flat, as shown in 1 groove. When the milling distance increased, the bottom of 3 and 5 grooves could not maintain the regular arc shape, and the side wall was no longer flat. As shown in Fig. 8c, the bottom of the microgroove milled with the PCD tool was flat, and no significant change was observed in the
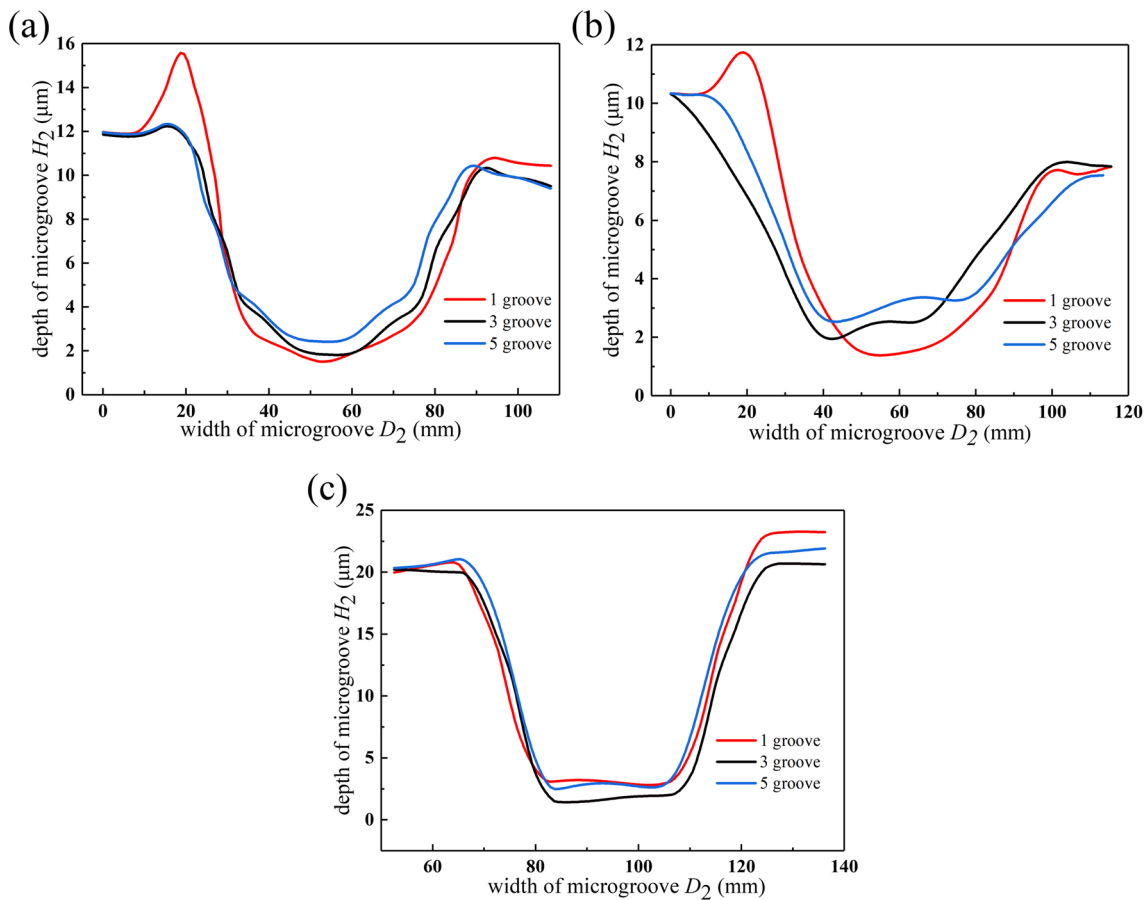
Fig. 8 The profile of microgrooves milled using a carbide tool, PCD-coated carbide tool, and PCD tool. (**a**) Carbide tool; (**b**) PCD-coated carbide tool; and (**c**) PCD tool

verticality of the side wall. As the milling distance increased, the groove type was consistent, indicating that PCD tool has the ability to achieve high-quality sidewall and groove bottom machining.
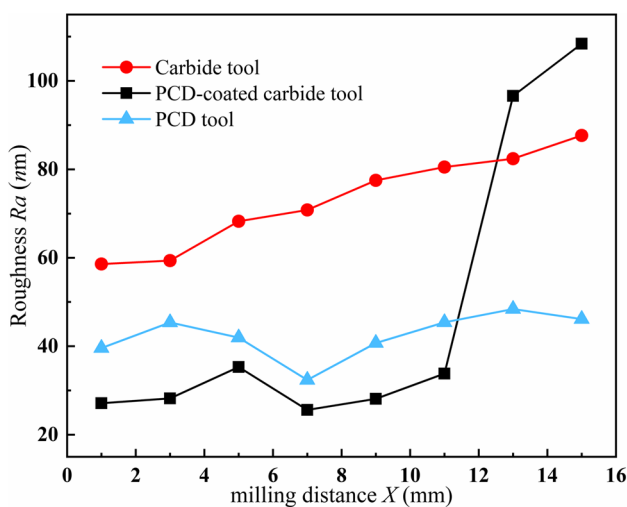
3.2.3 Microgroove surface roughness

The surface finish is critical in precision machining. Thus, studying the surface roughness of the processed material is necessary. To determine the influence of the carbide tool and PCD tool on the surface roughness of the groove bottom, the roughness change rate was evaluated, which can be expressed as

$$I_{Ra} = \frac{\bar{Ra}_{car} - \bar{Ra}_{PCD}}{\bar{Ra}_{car}} \qquad (2)$$

Where I_{Ra} is the roughness change rate, $\bar{Ra}_{car}$ represents the average roughness of the groove bottom milled carbide tool, and $\bar{Ra}_{PCD}$ represents the average roughness of the groove bottom milled PCD tool.

Figure 9 shows the variation in the groove bottom roughness with the milling distance under three kinds of tool milling. At the initial milling stage, the surface roughnesses of the carbide, PCD-coated carbide, and PCD tools were 58, 27, and 39 Ra, respectively. The roughness of the carbide tool is almost twice that of the PCD-coated carbide tool. The roughness linearly increased with the increase in milling distance. The roughness of the groove bottom milled with the PCD-coated carbide tool did not significantly change when the milling distance was within the range of 0–11 mm; however, when the milling distance exceeded 11 mm, the roughness of the groove bottom

Fig. 9 Surface roughness of milled groove bottom captured using a white light interferometer

significantly increased (more than three times). The poor surface quality of microgrooves milled using the PCD-coated carbide tool can be attributed to chips and peeled coatings accumulated on the machined surface and uneven distribution of material flow on the machined surface due to the prevalence of plowing, resulting in burr formation. The roughness of the microgroove bottom milled with the PCD tool slightly fluctuated, and the minimum roughness of 31.9 nm was achieved. Compared with the carbide tool, the surface roughness of the PCD tool was reduced by 41.9%. Therefore, the PCD tool can significantly improve the workpiece surface machining accuracy.

4 Conclusion

In summary, this paper presents an experimental study on the cutting performance of a 50-μm class of D-type carbide, PCD-coated carbide, and PCD tools during the brass micro-milling process. In addition, this paper describes the in situ preparation and milling of micro-milling tools. It also demonstrates that the application of micro-milling tools with a diameter of 50 μm class can expand the machining size range of ultra-precision micro-milling and improve the machining accuracy with small geometric features. The cutting performance was determined in terms of surface roughness, tool wear, rate of change in groove depth and width, burr formation, and surface topography. The following main conclusions were drawn:

(1) Compared with uncoated, the PCD micro-milling tool exhibited high-precision machining capabilities during brass milling. The PCD micro-milling tool produced relatively small top burrs. The surface roughness of the groove bottom milled with the PCD tool was 41.9% lower than that of the carbide tool, with a minimum roughness of 32.37 nm. When the milling distance of the PCD-coated carbide tool exceeded 11 mm, the coating fell off, and the surface roughness of the PCD-coated carbide tool sharply increased.

(2) Compared with uncoated and coated PCD carbide tools, the PCD tool had the longest service life. The cutting edge of the PCD tool remained intact after a cutting distance of 15 mm. Moreover, the maximum change rates of width and depth of the machined microgroove were the lowest, which were 0.18% and 4.9%, respectively.

(3) The microgrooves machined with PCD tools exhibited good groove retention. The groove shape was almost rectangular. However, the side walls and bottoms milled using uncoated and coated PCD carbide tools lost flatness after a cutting distance of 9 mm.

Hence, the PCD micro-milling tools exhibited good machining capability, which extended the tool life. This research has thrown up one question in need of further investigation. The milling performance of PCD micro-milling tools with a diameter of 50 μm on different materials still needs to be verified.

Author contribution All authors contributed to the study conception and design. Material preparation, data collection and analysis were performed by [Jiang Chen], [Rui Gao], [Hao Yu]. The first draft of the manuscript was written by [Jiang Jinxin] and all authors commented on previous versions of the manuscript. All authors read and approved the final manuscript.

Declarations

Competing interests The authors declare no competing interests.

References

1. Sun ZW, To S, Zhang S (2018) Theoretical and experimental investigation into non-uniformity of surface generation in micro-milling. Int J Mech Sci 140:313–324. https://doi.org/10.1016/j.ijmecsci.2018.03.019

2. Aramcharoen A, Mativenga PT, Yang S, Cooke KE, Teer DG (2016) Evaluation and selection of hard coatings for micro milling of hardened tool steel. Int J Mach Tool Manuf 48:1578–1584. https://doi.org/10.1016/j.ijmachtools.2008.05.011

3. Mittal RK, Singh RK, Kulkarni SS, Kumar P, Barshilia HC (2018) Characterization of anti-abrasion and anti-friction coatings on micromachining response in high speed micromilling of Ti-6Al-4V. J Manuf Process 34:303–312. https://doi.org/10.1016/j.jmapro.2018.06.021

4. Zhang EW, Yu TB, Zhao J (2020) Surface generation modeling of micro milling process with stochastic tool wear. Precis Eng 61:170–181. https://doi.org/10.1016/j.precisioneng.2019.10.015

5. Lu XH, Jia ZY, Wang H et al (2016) Tool wear appearance and failure mechanism of coated carbide tools in micro-milling of Inconel 718 super alloy. Ind Lubr Tribol 68:267–277. https://doi.org/10.1108/ILT-07-2015-0114

6. Silva LC, Silva M (2019) Investigation of burr formation and tool wear in micromilling operation of duplex stainless steel. Precis Eng 60:178–188. https://doi.org/10.1016/j.precisioneng.2019.08.006

7. Sahoo P, Patra K, Szalay T, Dyakonovet AA (2020) Determination of minimum uncut chip thickness and size effects in micro-milling of P-20 die steel using surface quality and process signal parameters. Int J Adv Manuf Technol 6(10):4675–4691. https://doi.org/10.1007/s00170-020-04926-6

8. Sahoo P, Patra K (2021) Cumulative reduction of friction and size effects in micro milling through proper selection of coating thickness of TiAlN coated tool: experimental and analytical assessments. J Manuf Process 67:635–654. https://doi.org/10.1016/j.jmapro.2021.05.037

9. Schneider M, Safonow E, Junker N et al (2017) Electrochemical machining of a solid-state sintered ceramic–a parameter study. Int J Refract Met H 68:19–23. https://doi.org/10.1016/j.ijrmhm.2017.06.004

10. Uhlmann E, Schauer K (2005) Dynamic load and strain analysis for the optimization of micro end mills. Cirp Ann-Manuf Techn 54:75–78. https://doi.org/10.1016/S0007-8506(07)60053-5

11. Perveen A, San WY, Rahman M (2012) Fabrication of different geometry cutting tools and their effect on the vertical micro-grinding of BK7 glass. Int J Adv Manuf Technol 61:101–115. https://doi.org/10.1007/s00170-011-3688-5

12. Sahoo P, Patra K (2019) Mechanistic modeling of cutting forces in micro-end-milling considering tool run out, minimum chip thickness and tooth overlapping effects. Mach Sci Technol 23:407–430. https://doi.org/10.1080/10910344.2018.1486423

13. Sorgato M, Bertolini R, Bruschi S (2020) On the correlation between surface quality and tool wear in micro–milling of pure copper. J Manuf Process 50:547–560. https://doi.org/10.1016/j.jmapro.2020.01.015

14. Souza PS, Santos AJ, Cotrim M, Abro AM, Cmara MA (2020) Analysis of the surface energy interactions in the tribological behavior of ALCrN and TIAlN coatings. Tribol Int 146:106206. https://doi.org/10.1016/j.triboint.2020.106206

15. Kumar AS, Deb S, Paul S (2020) Tribological characteristics and micromilling performance of nanoparticle enhanced water based cutting fluids in minimum quantity lubrication. J Manuf Processes 56:766–776. https://doi.org/10.1016/j.jmapro.2020.05.032

16. Zhao G, Li Z, Hu ZY, Li MS, He L, Muhammad NJ (2019) Fabrication and performance of CVD diamond cutting tool in micro milling of oxygen-free copper. Diamond Relat Mater 100:107589. https://doi.org/10.1016/j.diamond.2019.107589

17. Wang Y, Zou B, Wang J, Wu Y, Huang C (2020) Effect of the progressive tool wear on surface topography and chip formation in micro-milling of Ti–6Al–4V using Ti (C7N3)-based cermet micro-mill. Tribol Int 141:105900. https://doi.org/10.1016/j.triboint.2019.105900

18. Thepsonthi T, Özel T (2013) Experimental and finite element simulation based investigations on micro-milling Ti-6Al-4V titanium alloy: effects of cBN coating on tool wear. J Mater Process Technol 213:532–542. https://doi.org/10.1016/j.jmatprotec.2012.11.003

19. Farrukh H, Deviprakash JD, Jamal SA, Almaskari F (2022) Wear mechanism and quantification of polycrystalline diamond milling cutter in high speed trimming of carbon fiber reinforced epoxy. Int J Refract Met H 106:105863. https://doi.org/10.1016/j.ijrmhm.2022.105863

20. Cheng X, Wang ZG, Nakamoto K et al (2011) A study on the micro tooling for micro/nano milling. Int J Adv Manuf Technol 53:523–533. https://doi.org/10.1007/s00170-010-2856-3

21. Aurich JC, Kieren ES, Mayer T, Bohley M (2022) An investigation of the influence of the coating on the tool lifetime and surface quality for ultra-small micro end mills with different diameters. CIRP Ann-Manuf Techn 37:92–102. https://doi.org/10.1016/j.cirpj.2022.01.004

22. Ding L, Zhang H, Sha XQ (2022) Experimental investigation on helium valved linear compressors with different active offsets. Cryogenics 124:103483. https://doi.org/10.1016/j.cryogenics.2022.103483

23. Aslantas K, Hopa HE, Percin M, Ucun A, Icek AB (2016) Cutting performance of nano-crystalline diamond (NCD) coating in micro-milling of Ti 6 Al 4 V alloy. J Precis Eng 45:55–66. https://doi.org/10.1016/j.precisioneng.2016.01.009

24. Liang Z, Gao P, Wang X, Li S, Zhou T, Xiang J (2018) Cutting performance of different coated micro end mills in machining of Ti-6Al-4V. J Micromachines 9:568–579. https://doi.org/10.3390/mi9110568

25. Roushan A, Rao US, Patra K, Sahoo P (2022) Performance evaluation of tool coatings and nanofluid MQL on the micro-machinability of Ti-6Al-4V. J Manuf Processes 73:595–610. https://doi.org/10.1016/j.jmapro.2021.11.030